Production Processes and Properties of Powders
Процессы получения и свойства порошков

UDC 546.261'82'74-047.84-022.532
https://doi.org/10.17073/1997-308X-2024-3-5-15

Research article
Научная статья

Plasma-chemical synthesis of highly dispersed core–shell structures from a mechanical mixture of titanium carbide and titanium nickelide

Yu. A. Avdeeva[1], I. V. Luzhkova[1], A. M. Murzakaev[2], A. N. Ermakov[1]

[1] **Institute of Solid State Chemistry, Ural Branch, Russian Academy of Sciences**
91 Pervomaiskaya Str., Yekaterinburg, Sverdlovsk Region 620990, Russia
[2] **Institute of Electrophysics, Ural Branch, Russian Academy of Sciences**
106 Amundsen Str., Yekaterinburg, Sverdlovsk Region 620216, Russia

y-avdeeva@list.ru

Abstract. In this paper, we studied the formation of ultrafine and nanocrystalline core–shell structures based on refractory compounds of titanium with nickel during plasma-chemical synthesis of a mechanical mixture of TiC and TiNi in a low-temperature nitrogen plasma. Cooling took place in an intensely swirling nitrogen flow in a quenching chamber. The derived products were separated in a vortex-type cyclone and a bag-type fabric filter. After processing, the products were subjected to encapsulation aimed at reducing the pyrophoricity for long-term storage of the resulting finely dispersed powders under normal conditions. *X*-ray diffraction and high-resolution transmission electron microscopy were used to study the resulting powder products of plasma-chemical synthesis, and density measurements were conducted. Additionally, to define the average particle size more accurately, the specific surface was measured using the BET method. The instrumental research revealed the presence of ultra- and nanodispersed particles with a core–shell structure in the powder products. These particles included titanium carbide-nitride compounds as a refractory core and metallic nickel as a metallic shell. In addition, the presence of complex titanium-nickel nitride $Ti_{0.7}Ni_{0.3}N$ was recorded. According to direct measurements, the average particle size of the nanocrystalline fraction is 18.9 ± 0.2 nm. The obtained research results enabled us to develop a chemical model of crystallization of TiC_xN_y–Ni core–shell structures, which is implemented in a hardening chamber at a crystallization rate of 10^5 °C/s. To fabricate the model, we used the reference data on the boiling and crystallization temperatures of the elements and compounds being a part of highly dispersed compositions and recorded by *X*-ray diffraction, as well as the $\Delta G(t)$ dependences for TiC and TiN.

Keywords: titanium nickelide, titanium carbide, plasma-chemical synthesis, low-temperature plasma, *X*-ray phase analysis, high-resolution transmission electron microscopy

Acknowledgements: The work was carried out in accordance with the state assignment for the Institute of Solid State Chemistry of the Ural Branch of the Russian Academy of Sciences (theme No. 24020600024-5).

For citation: Avdeeva Yu.A., Luzhkova I.V., Murzakaev A.M., Ermakov A.N. Plasma-chemical synthesis of highly dispersed core–shell structures from a mechanical mixture of titanium carbide and titanium nickelide. *Powder Metallurgy and Functional Coatings*. 2024;18(3):5–15. https://doi.org/10.17073/1997-308X-2024-3-5-15

Плазмохимический синтез высокодисперсных структур «ядро–оболочка» из механической смеси карбида титана с никелидом титана

Ю. А. Авдеева[1], И. В. Лужкова[1], А. М. Мурзакаев[2], А. Н. Ермаков[1]

[1] Институт химии твердого тела УрО РАН
Россия, 620990, Свердловская обл., г. Екатеринбург, ул. Первомайская, 91
[2] Институт электрофизики УрО РАН
Россия, 620216, Свердловская обл., г. Екатеринбург, ул. Амундсена, 106

y-avdeeva@list.ru

Аннотация. Проведены исследования, направленные на формирование ультрадисперсных и нанокристаллических структур «ядро–оболочка» на основе тугоплавких соединений титана с никелем в ходе плазмохимического синтеза механической смеси TiC и TiNi в низкотемпературной азотной плазме. Охлаждение происходило в интенсивно закрученном потоке газообразного азота в закалочной камере. Продукты переработки сепарировались в условиях циклона вихревого типа и тканевого фильтра рукавного типа. После переработки продукты подвергались капсулированию, направленному на понижение пирофорности для длительного хранения полученных высокодисперсных порошков в нормальных условиях. Переработанные порошковые продукты плазмохимического синтеза исследовались методами рентгенографии, просвечивающей электронной микроскопии высокого разрешения и измерения плотности. Дополнительно, для уточнения среднего размера частиц, проводились измерения удельной поверхности по методике BET. Результаты аппаратурных исследований показали наличие ультра- и нанодисперсных частиц со структурой «ядро–оболочка» в порошковых продуктах. Эти частицы включали карбидно-нитридные соединения титана в качестве тугоплавкого ядра и металлический никель в виде металлической оболочки. Дополнительно зафиксировано присутствие сложного титан-никелевого нитрида $Ti_{0,7}Ni_{0,3}N$. Нанокристаллическая фракция по результатам прямых измерений характеризуется средним размером частиц 18,9 ± 0,2 нм. На основе полученных результатов исследований была сформирована химическая модель кристаллизации структур «ядро–оболочка» TiC_xN_y–Ni, реализуемая в условиях закалочной камеры со скоростью кристаллизации 10^5 °C/c. Для составления модели использовались справочные данные о температурах кипения и кристаллизации элементов и соединений, входящих в состав высокодисперсных композиций и зафиксированных рентгенографически, а также зависимости $\Delta G(t)$ для TiC и TiN.

Ключевые слова: никелид титана, карбид титана, плазмохимический синтез, низкотемпературная плазма, рентгенофазовый анализ, просвечивающая электронная микроскопия высокого разрешения

Благодарности: Работа выполнена в соответствии с государственным заданием Института химии твердого тела УрО РАН (тема № 124020600024-5).

Для цитирования: Авдеева Ю.А., Лужкова И.В., Мурзакаев А.М., Ермаков А.Н. Плазмохимический синтез высокодисперсных структур «ядро–оболочка» из механической смеси карбида титана с никелидом титана. *Известия вузов. Порошковая металлургия и функциональные покрытия*. 2024;18(3):5–15. https://doi.org/10.17073/1997-308X-2024-3-5-15

Introduction

At present, the nanocrystalline state of matter is extensively investigated [1–5] as it has a number of unique physicochemical and physicomechanical properties determined by the high dispersion of particles. For example, the most productive methods for the formation of nanocrystalline materials include plasma-chemical synthesis in a low-temperature gas plasma [6]. From the standpoint of fundamental research [7], "quasi-equilibrium" processes occurring during plasma-chemical synthesis in a low-temperature gas plasma enable one to use the laws of equilibrium thermodynamics to calculate the final state of the reacting system.

The formation of core–shell structures of a given composition during synthesis of ultra- and nanodisperse materials based on refractory compounds of IV–VIA subgroups of the periodic table, with the participation of metals such as Ni and Co, makes it possible to synthesize composite powder products suitable for direct use. One of the technological examples is the use of nanomaterials, obtained during plasma-chemical synthesis in a low-temperature nitrogen plasma and based on refractory compounds of titanium, vanadium, zirconium and other elements of IV–VIA subgroups, as modifiers for casting steels and non-ferrous alloys, as described in [8–10]. During extra-furnace steel processing, nanocrystalline materials are placed into a ladle using different methods and are rather evenly distributed throughout the molten steel or non-ferrous alloy, acting as artificial nuclei during crystallization. The metal components of composite nanocrystalline

particles, therefore, serve as a buffer layer between the melt and the refractory core, protecting the latter from early solid-phase dissolution. The microquantities of such modifiers improve the physical and mechanical properties of cast materials while maintaining their specified chemical composition.

On the other hand, refractory compounds based on elements of IV–VIA subgroups of the periodic table, with high hardness values, are used as the basis for tool materials [11]. The binding phases are metals and their intermetallic compounds, which allow metal ceramic compositions to be formed, where the matrix in the form of grains of refractory compounds is impregnated with a metal melt during high-temperature sintering in vacuum with the participation of a liquid phase. The patterns of such processes for various powder compositions based on titanium carbonitride $TiC_{0.5}N_{0.5}$ were earlier described in [12–16].

The main objective of this paper is to study the patterns for the formation of ultradisperse and nanocrystalline particles with a core–shell structure during plasma-chemical synthesis of a mechanical mixture of TiC and TiNi (1:1) in a low-temperature nitrogen plasma.

Methods

Microcrystalline powders of titanium carbide (50 μm) and titanium nickelide (40 μm) were used as the initial components of the charge for plasma-chemical synthesis. The industrial plasma-chemical plant described in [6] was used for plasma-chemical synthesis. The plant productivity can reach 1 t/h, which confirms a quite reasonable cost of this technology.

The capacity of the plasma chemical plant (FSUE SRIOCCT, Saratov) was 25 kW, voltage – 200–220 V, current – 100–110 A, plasma flow speed – 55 m/s, gaseous nitrogen flow rate in the plasma reactor – 25–30 m^3/h (of which plasma formation accounted for 6 m^3/h and stabilization and hardening – 19–24 m^3/h). The initial mechanical mixture consumption was 200 g/h.

The pneumatic transport transferred the processed ultrafine and nanocrystalline powder into a vortex-type cyclone and a bag-type fabric filter for separation. Nitrogen was used as a transport gas. After cooling, air was slowly introduced into the separation units to form a thin passivating oxide film. At the next passivation stage, the materials were encapsulated in a specialized unit of a plasma-chemical plant (capsulator), which ensures long-term storage of highly dispersed materials under normal conditions. The technique of plasma-chemical synthesis in a low-temperature nitrogen plasma based on the plasma recondensation scheme is described in more detail in [6].

The core–shell structures processed in the form of ultrafine and nanocrystalline powders were studied by *X*-ray diffraction (SHIMADZU XRD 7000 *X*-ray diffractometer, CuK_α-cathode, Japan) and high-resolution transmission electron microscopy (HR TEM) (JEOL JEM 2100 transmission electron microscope, Japan). The *X*-ray investigation results were processed using the WinXPOW software (ICDD database) to determine the phase composition of the resulting core–shell structures. The crystallographic parameters of the phase components were specified in the PowderCell 2.3 software package using the ICSD file located on the Springer Materials e-platform. The electron microscope images were processed to measure particle sizes in Measurer software and then in standard mathematical editors to construct distribution histograms and determine the average particle size. High-resolution images were processed in the DigitalMicrograph 7.0 software. The results of interplanar spacing measurements were compared with the ICDD database file to specify the phase composition and determine the local states of additionally detected phases.

The density of the final synthesis products was assessed using a helium pycnometer (AccuPyc II 1340 V1.09, Micromeritics, USA). The specific surface area was measured on a specific surface area analyzer (Gemini VII 2390 V1.03 (V1.03 t), USA) using the BET method. The average particle size was determined for each of the processed fractions based on the values of density and specific surface area [17].

Results and discussion

The results of *X*-ray investigations of fractions of core-shell structures obtained during plasma-chemical synthesis in a low-temperature nitrogen plasma of a mechanical mixture of TiC and TiNi are presented in Fig. 1 and in the table. The refractory phase in both fractions of dispersed materials is represented by cubic compounds.

While specifying the unit cell parameters, we revealed that during crystallization in a quenching chamber at a rate of 10^5 °C/s, oxycarbide and carbonitride phases of various compositions are formed in each fraction, as indicated in the table. The carbonitride composition is formed with a predominant amount of nitrogen in the non-metallic sublattice.

According to *X*-ray diffraction results, the cubic Ni phase (*Fm*-3*m* space group) is observed only in the fabric filter fraction, where its amount is determined to be 5 wt. % (see the Table). At the same time, the *X*-ray diffraction pattern of the powder composi-

tion from the filter contains complex titanium-nickel nitride $Ti_{0.7}Ni_{0.3}N$ in the amount of 5 wt. %. According to the *X*-ray diffraction patterns (see Fig. 1), titanium-nickel nitride $Ti_{0.7}Ni_{0.3}N$, the visualization of which was presented in [18], is in a highly deformed state causing changes in intensities [19]. The resulting preferential orientation of the crystal lattice, in accordance with [20], can be ensured by the high rate of crystallization of the obtained powders. The issues related to formation and identification of $Ti_{0.7}Ni_{0.3}N$ using the example of the TiN–Ni core–shell structure, studied within the framework of high-resolution transmission electron microscopy, are discussed in [21]. The rutile modification of TiO_2 is formed in the course of forced acidification by slow inflow of air into classifiers *1* and *2*, its share being 2 wt. %.

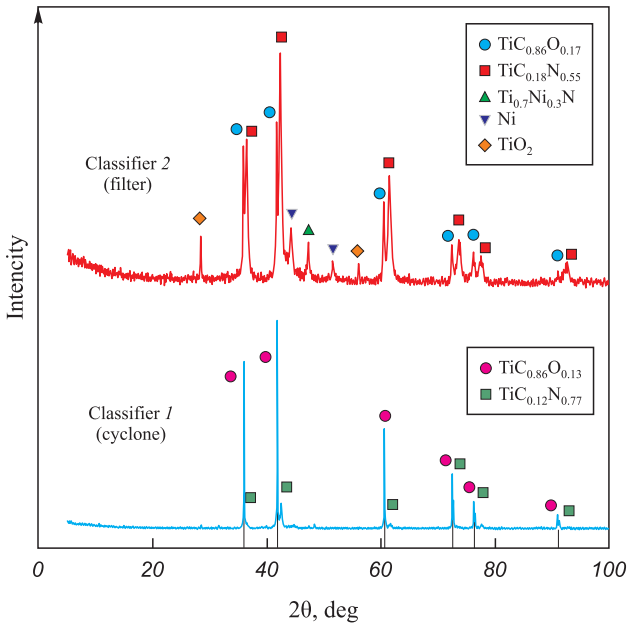

Fig. 1. *X*-ray diffraction patterns of highly dispersed fractions obtained from a mechanical mixture of TiC and TiNi (1:1) during plasma-chemical synthesis in a low-temperature nitrogen plasma

Рис. 1. Рентгенограммы высокодисперсных фракций, полученных из механической смеси TiC–TiNi (1:1) в процессе плазмохимического синтеза в низкотемпературной азотной плазме

The measurements of pycnometric density and specific surface area by the BET method, presented in the table, revealed that the core–shell structures formed differ in density values. This effect can be attributed to the quantitative content of the processed compositions.

Visualization of the core–shell structure using the example of a nanocrystalline fraction from classifier *2* – a bag-type fabric filter – was confirmed by high-resolution transmission electron microscopy (Fig. 2).

Figure 2, *a*, *b* shows the general picture, which demonstrates that the fraction from the filter is really nanodispersed, since the average particle size based on the results of 767 measurements is 18.9 ± 0.2 nm; the histogram of particle size distribution is shown in Fig. 2, *c*.

The presence of a core–shell structure is determined by the presence of high-contrast areas at the periphery of the grains, and the grains themselves have both a round and faceted shape, as shown in Fig. 3.

Figure 3 shows the results of fixation of metallic nickel (plot *1*) and titanium carbide TiC (plot *2*). According to the results of measurements of interplanar spacing in plot *1*, cubic metallic Ni (*Fm*-3*m*

Phase composition, density (ρ), specific surface area (S_{sp}) and the calculated value of the average size of the resulting particles (d_{avg}) from the mechanical mixture of TiC and TiNi (1:1) after plasma-chemical synthesis in a low-temperature nitrogen plasma

Фазовый состав, плотность (ρ), удельная поверхность ($S_{уд}$) и расчетное значение среднего размера полученных частиц ($d_{ср}$) из механической смеси TiC–TiNi (1:1) после плазмохимического синтеза в низкотемпературной азотной плазме

Fraction	Phase composition	Space group	Phase fraction, wt. %	Lattice parameter, nm	ρ, g/cm³	S_{sp}, m²/g	d_{avg}, μm
Classifier *1* (cyclone)	$TiC_{0.86}O_{0.13}$	*Fm*-3*m*	86	*a* = 0.43162	5.99	5.27	0.19
	$TiC_{0.12}N_{0.77}$	*Fm*-3*m*	14	*a* = 0.42496			
Classifier *2* (filter)	TiC	*Fm*-3*m*	44	*a* = 0.43222	5.66	106.00	0.01
	$TiC_{0.18}N_{0.55}$	*Fm*-3*m*	44	*a* = 0.42606			
	Ni	*Fm*-3*m*	5	*a* = 0.35406			
	TiO_2	*P*42/*mnm*	2	*a* = 0.44860			
				c = 0.29859			
	$Ti_{0.7}Ni_{0.3}N$	*P*-6*m*2	5	*a* = 0.29735			
				c = 0.28934			

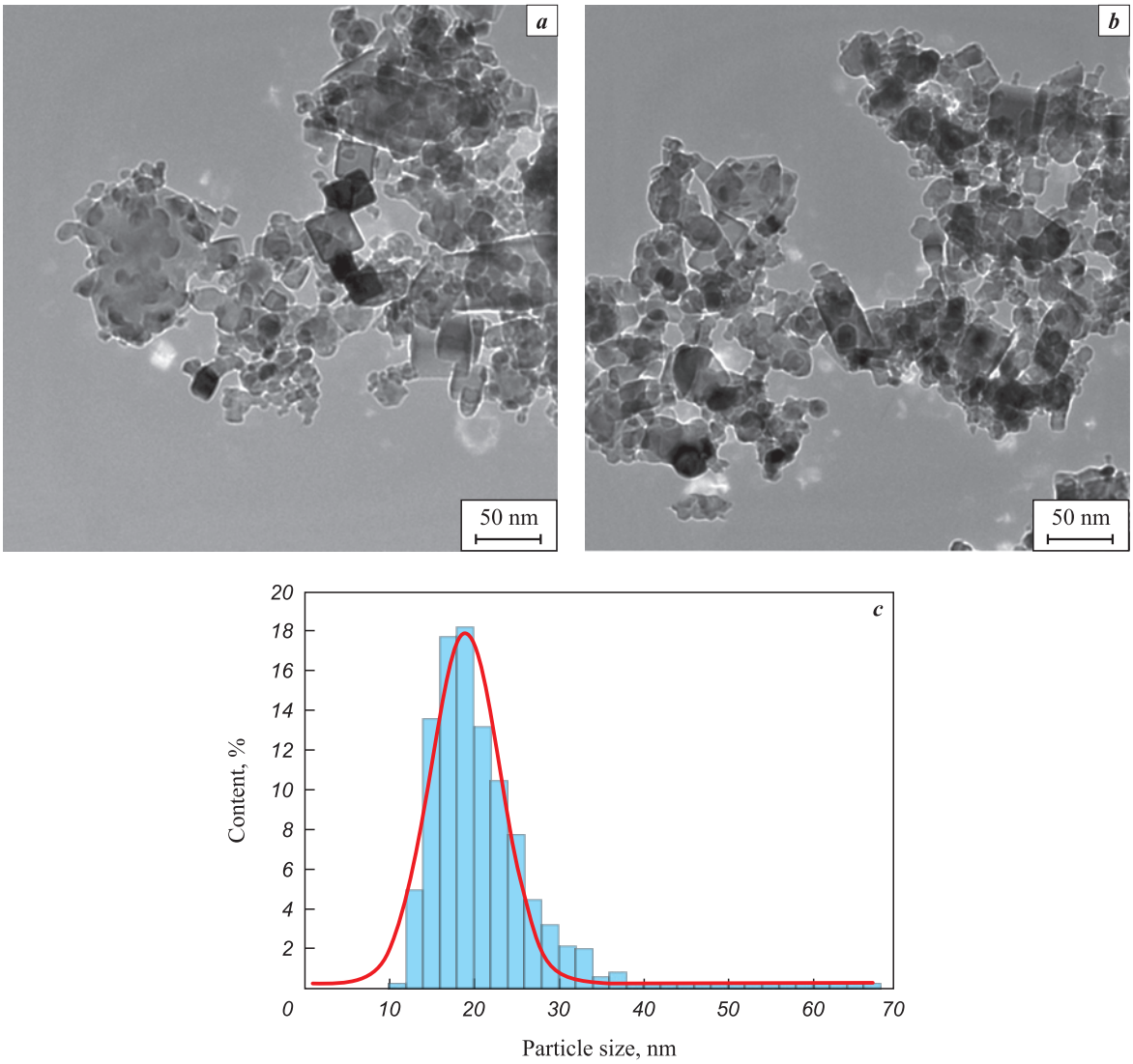

Fig. 2. HR TEM of a nanocrystalline powder with a core–shell structure obtained from a powder mechanical mixture of TiC and TiNi (1:1) during plasma-chemical synthesis in a low-temperature nitrogen plasma (***a***, ***b***) and histogram of particle size distribution plotted based on direct measurements (***c***)

Рис. 2. ПЭМ ВР нанокристаллического порошка со структурой «ядро–оболочка», полученного из порошковой механической смеси TiC–TiNi (1:1) в ходе плазмохимического синтеза в низкотемпературной азотной плазме (***a***, ***b***), и гистограмма распределения размеров частиц, построенная на основе прямых измерений (***c***)

space group) is characterized by interplanar spacings $d_{200} = 0.1797$ nm, $d_{111} = 0.2054$ nm, and $d_{-111} = 0.2087$ nm. In plot *2*, the identified planes belong to TiC (*Fm*-3*m* space group), $d_{111} = 0.2533$ nm.

The hexagonal Ni is present in the form of a (002) plane with interplanar spacing $d_{002} = 0.2189$ nm in the section of the electron microscope image shown in Fig. 4.

The presence of titanium-nickel nitride $Ti_{0.7}Ni_{0.3}N$ of the hexagonal modification (*P*-6*m*2 space group, $d_{100} = 0.2543$ nm) along with hexagonal Ni (space group $P6_3/mmc$, $d_{100} = 0.2250$ nm) and cubic TiC (*Fm*-3*m* space group, $d_{111} = 0.2568$ nm) is shown in Fig. 5.

Based on the TEM studies, Fig. 6 shows an example of the presence of faceted particles of cubic titanium carbide TiC – the composition of the presented faceted particle is interpreted by the (200) TiC plane (*Fm*-3*m* space group), $d_{200} = 0.2150$ nm.

Summarizing the findings of *X*-ray diffraction and high-resolution transmission electron microscopy, we can formulate a chemical model of the core–shell structures formed during plasma-chemical synthesis in a low-temperature nitrogen plasma followed by crystallization in an intensely swirling nitrogen flow (Fig. 7). The model is based on the physicochemical properties of all interpreted phase components, which include boiling, condensation and crystallization tem-

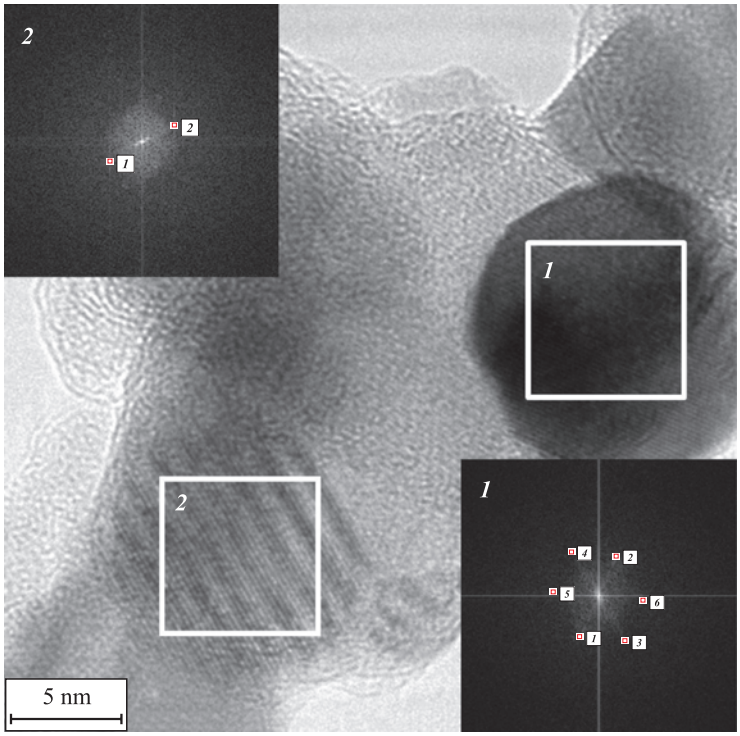

Fig. 3. HR TEM of nanocrystalline powder particles with a core–shell structure obtained from a powder mechanical mixture of TiC and TiNi (1:1) during plasma-chemical synthesis in a low-temperature nitrogen plasma, taking into account the presence of metallic Ni (plot *1*) and titanium carbide TiC (plot *2*)

Рис. 3. ПЭМ ВР нанокристаллических частиц порошка со структурой «ядро–оболочка», полученного из порошковой механической смеси TiC–TiNi (1:1) в ходе плазмохимического синтеза в низкотемпературной азотной плазме, с учетом присутствия металлического Ni (участок *1*) и карбида титана TiC (участок *2*)

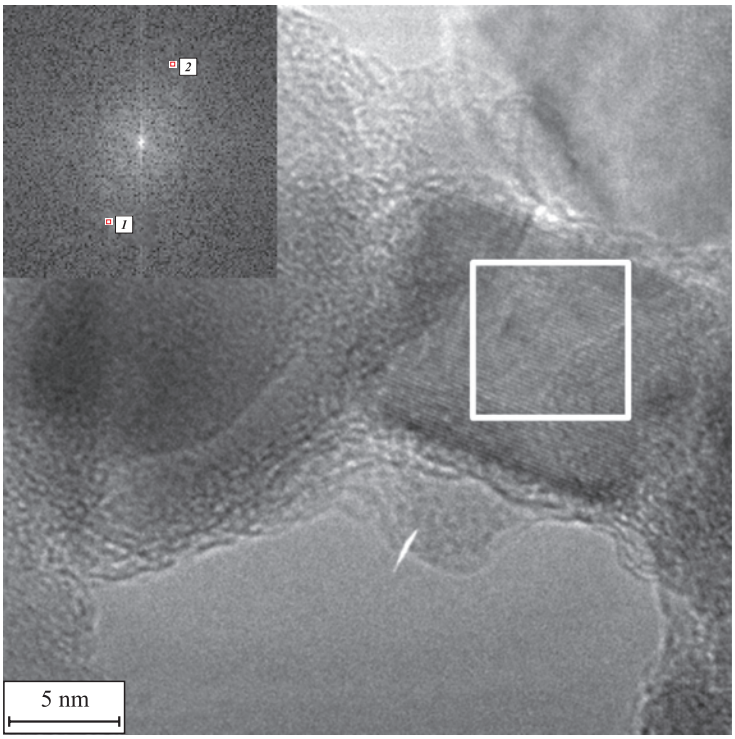

Fig. 4. Localized state of hexagonal metallic Ni according to the results of HR TEM and fast Fourier transform

Рис. 4. Локализованное состояние металлического Ni гексагональной модификации по результатам ПЭМ ВР и быстрого преобразования Фурье

peratures [22; 23], as well as functional dependences $\Delta G(t)$ under equilibrium conditions [24]. Additionally, information on the wettability of refractory compounds [22] by molten nickel metal was utilized to justify the metallic shell on the periphery of nanocrystalline refractory particles.

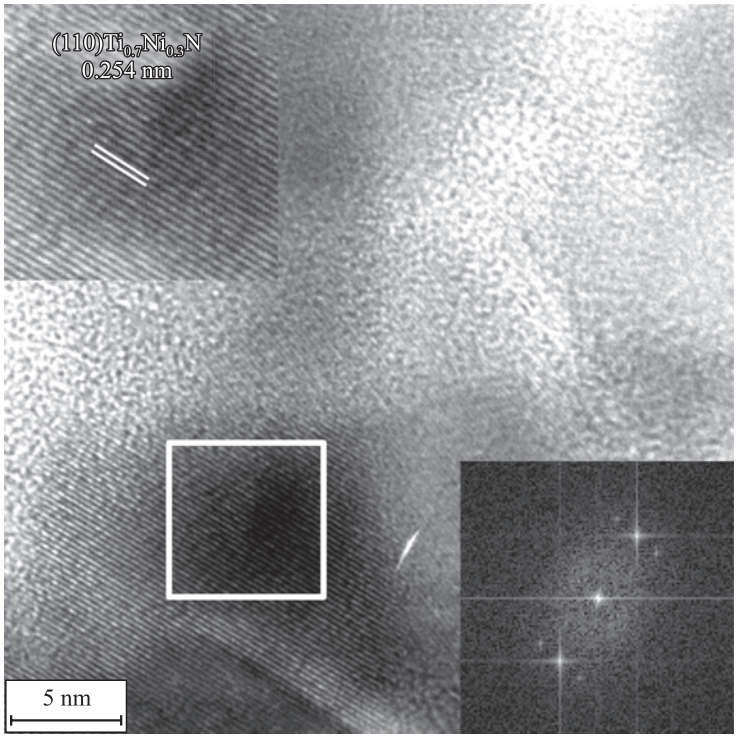

Fig. 5. Localized state of $Ti_{0.7}Ni_{0.3}N$ (*P*-6*m*2 space group) according to the results of HR TEM

Рис. 5. Локализованное состояние $Ti_{0,7}Ni_{0,3}N$ (пр. гр. *P*-6*m*2) по результатам ПЭМ ВР

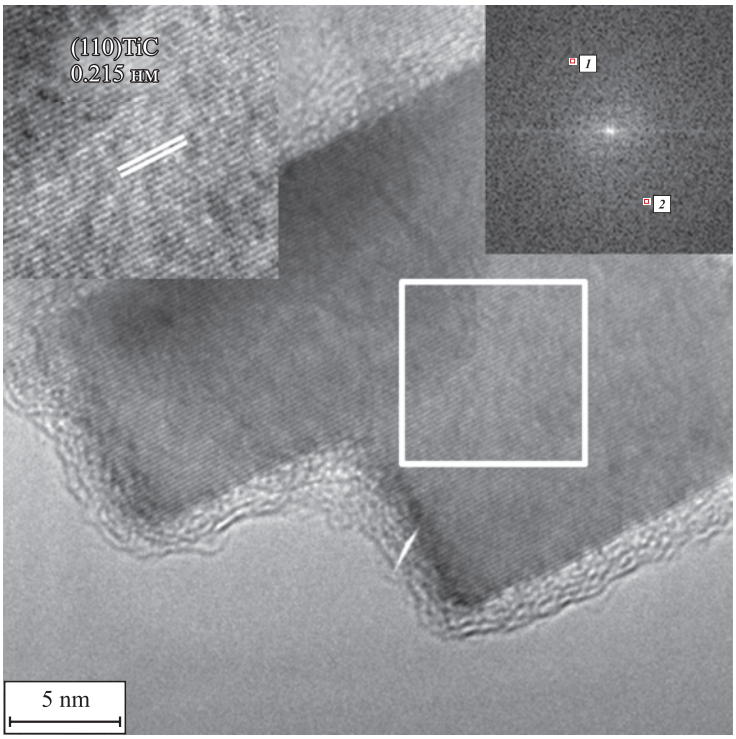

Fig. 6. Faceted nanocrystalline TiC particle coated with an amorphous layer of metallic nickel

Рис. 6. Ограненная нанокристаллическая частица TiC, покрытая аморфным слоем металлического никеля

Within the framework of this model, the flow of low-temperature plasma with a mechanical mixture of TiC and TiNi is separated by temperature barriers as it enters the quenching chamber filled with nitrogen. The boiling or crystallization temperatures of all phase components determined by *X*-ray diffraction are selected as temperature barriers.

Keeping in mind that low-temperature plasma can exist only in the temperature range of 4000–6000 °C, the first temperature barrier responsible for the crystallization of the refractory components of the emerging core–shell structures can be identified as the transition of titanium carbide from a gaseous state to a solid state described in [25–28], its temperature is 4300 °C [23]. Considering the significant excess of gaseous nitrogen in the entire volume of the quenching chamber, it can be stated that under these conditions it interacts with solid-phase TiC with the subsequent formation of carbonitride TiC_xN_z (see the Table). The functional dependences $\Delta G(t)$ for these processes [24] and the data on phase formation in the Ti–C–N system [29] confirm that mutual solid solutions with wide homogeneity regions can be formed. At the same time, during the crystallization of refractory components in the quenching chamber, TiNy titanium nitride nanoparticles, isomorphic to Ti–C–N compounds, can be formed on the surface.

Separately, it should be mentioned that passing the temperature range of 4300–3930 °C nickel remains in a gaseous state up to the temperature of 2730 °C [30], at which it passes from a gaseous to a liquid state and which is the second temperature barrier. Passing the boiling point, liquid nickel actively interacts with refractory grains. Under these conditions, titanium-nickel nitride $Ti_{0.7}Ni_{0.3}N$ is formed [21] according to the theory of heterogeneous nucleation by B. Chalmers [31], some provisions of which are given in [8] by the reaction equation

$$TiN_y\,(s) + Ni\,(l) + N_2\uparrow \rightarrow Ti_{0.7}Ni_{0.3}N. \qquad (1)$$

It should be noted that the complex nitride $Ti_{0.7}Ni_{0.3}N$ and its analogue $Ti_{0.7}Co_{0.3}N$ were earlier detected by *X*-ray diffraction and transmission electron microscopy and described in [21; 32–34].

Reaction (1) occurs in the temperature range from 1600 °C [18] to 1455 °C, which corresponds to the crystallization temperature of metallic nickel and constitutes the third temperature barrier in the presented model. As nickel crystallizes, no chemical interactions occur in the formed core–shell structures, and all the resulting compositions can only cool down at this stage. Next, the mixture of processed fractions is transported to classifiers *1* and *2* for separation.

Conclusion

As a result of plasma-chemical synthesis in a low-temperature nitrogen plasma, we obtained ultrafine and nanocrystalline fractions of particles with a core–shell structure from a mechanical mixture of titanium carbide TiC and titanium nickelide TiNi in the ratio of 1:1.

All the resulting powder compositions were studied by *X*-ray diffraction and helium pycnometry. The specific surface area was determined using the BET method. The nanocrystal-

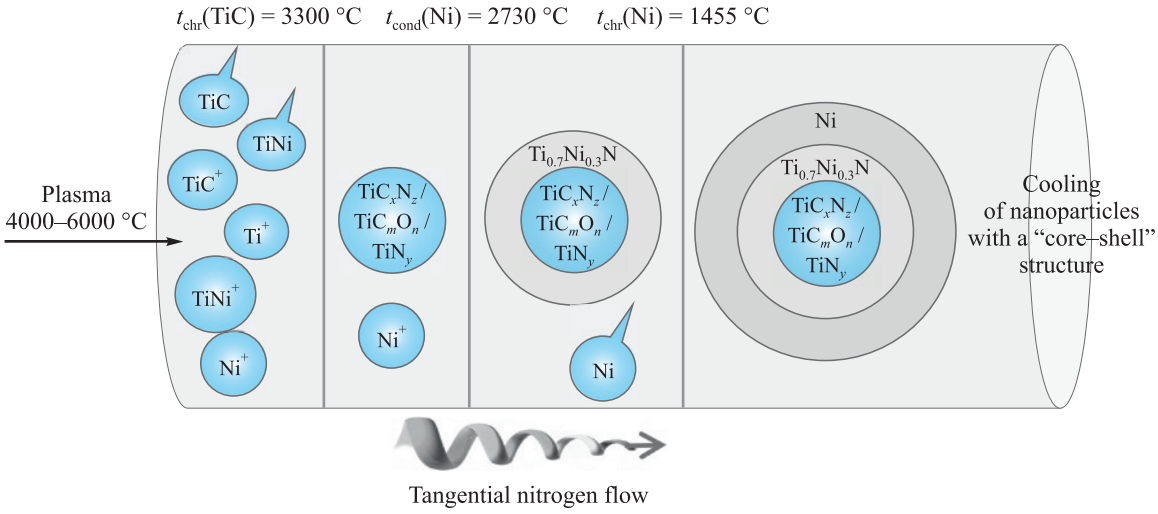

Fig. 7. Chemical mechanism of formation of a core–shell structure during plasma-chemical synthesis of the powder mixture of TiC and TiNi (1:1) in a low-temperature nitrogen plasma

Рис. 7. Химический механизм формирования структуры «ядро–оболочка» в ходе плазмохимического синтеза порошковой смеси TiC–TiNi (1:1) в низкотемпературной азотной плазме

line fraction was thoroughly investigated using high-resolution transmission electron microscopy.

Based on the research findings, the following conclusions can be drawn:

1. The ultra- and nanodispersed compositions formed during plasma-chemical synthesis have a core–shell structure. According to *X*-ray phase analysis confirmed by the results of high-resolution transmission electron microscopy, the refractory core is the $TiC/TiC_xN_y/TiC_xO_z$ compound coated with a metallic Ni shell; the complex titanium-nickel nitride $Ti_{0.7}Ni_{0.3}N$ acts as an interphase layer.

2. Based on *X*-ray diffraction and transmission electron microscopy data, taking into account the physicochemical features of the detected phase components, we formulated the chemical mechanism for the formation of ultradisperse and nanocrystalline particles with a core–shell structure under crystallization conditions at a rate of 10^5 °C/s in a tangential nitrogen flow in a quenching chamber of the plasmatron.

3. The chemical mechanism of the formation of nanocrystalline particles is the overcoming of temperature barriers by the plasma flow, with elements evaporated in it that are a part of the charge. The crystallization temperatures of phase components that are present, according to *X*-ray diffraction, in ultradisperse and nanocrystalline particles act as temperature barriers.

References / Список литературы

1. Song M., Yang Y., Xiang M., Zhu Q., Zhao H. Synthesis of nano-sized TiC powders by designing chemical vapor deposition system in a fluidized bed reactor. *Powder Technology*. 2021;380:256–264. https://doi.org/10.1016/j.powtec.2020.11.045
2. Dorosheva I.B., Vokhmintsev A.S., Weinstein I.A., Rempel A.A. Induced surface photovoltage in TiO_2 sol-gel nanoparticles. *Nanosystems: Physics, Chemistry, Mathematics*. 2023;14(4):447–453. https://doi.org/10.17586/2220-8054-2023-14-4-447-453
3. Kozlova T.O., Popov A.L., Romanov M.V., Savintseva I.V., Vasilyeva D.N., Baranchikov A.E., Ivanov V.K. Ceric phosphates and nanocrystalline ceria: selective toxicity to melanoma cells. *Nanosystems: Physics, Chemistry, Mathematics*. 2023;14(2):223–230. https://doi.org/10.17586/2220-8054-2023-14-2-223-230
4. Balestrat M., Cheype M., Gervais C., Deschanels X., Bernard S. Advanced nanocomposite materials made of TiC nanocrystals in situ immobilized in SiC foams with boosted spectral selectivity. *Materials Advances*. 2023;(4): 1161–1170.https://doi.org/10.1039/D2MA00886F
5. Kapusta K., Drygas M., Janik J.F., Olejniczak Z. New synthesis route to kesterite Cu_2ZnSnS_4 semiconductor nanocrystalline powders utilizing copper alloys and a high energy ball milling-assisted process. *Journal of Materials Research and Technology*. 2020;9(6):13320–13331. https://doi.org/10.1016/j.jmrt.2020.09.062
6. Storozhenko P.A., Guseinov Sh.L., Malashin S.I. Nanodispersed powders: Synthesis methods and practical applications. *Nanotechnologies in Russia*. 2009;4:262–274. https://doi.org/10.1134/S1995078009050024

   Стороженко П.А., Гусейнов Ш.Л., Малашин С.И. Нанодисперсные порошки: Методы получения и способы практического применения. *Российские нанотехнологии*. 2009;4(1–2):27–39. https://doi.org/10.1134/S1995078009050024
7. Tsvetkov Yu.V. Plasma metallurgy: current state, problems and prospects. *Pure and Applied Chemistry*. 1999;71(10): 1853–1862. https://doi.org/10.1351/pac199971101853
8. Zhukov M.F., Cherskiy I.N., Cherepanov A.N., Konovalov N.A., Saburov V.P., Pavlenko N.A., Galevskiy G.V., Andrianova O.A., Krushenko G.G. Hardening of metallic polymeric and elastomer materials by ultrafine powders of plasma-chemical synthesis. Novosibirsk: Nauka, 1999. 307 p. (In Russ.).

   Жуков М.Ф., Черский И.Н., Черепанов А.Н., Коновалов Н.А., Сабуров В.П., Павленко Н.А., Галевский Г.В., Андрианова О.А., Крушенко Г.Г. Упрочнение металлических полимерных и эластомерных материалов ультрадисперсными порошками плазмохимического синтеза. Новосибирск: Наука, 1999. 307 с.
9. Ermakov A.N., Luzhkova I.V., Avdeeva Yu.A., Dyakov A.A., Maurin N.I. Steel modification method: Patent 2781940 (RF). 2022. (In Russ.).

   Ермаков А.Н., Лужкова И.В., Авдеева Ю.А., Дьяков А.А., Маурин Н.И. Способ модифицирования стали: Патент 2781940 (РФ). 2022.
10. Ermakov A.N., Luzhkova I.V., Avdeeva Yu.A. Steel modification method: Patent 2781935 (RF). 2022. (In Russ.).

    Ермаков А.Н., Лужкова И.В., Авдеева Ю.А. Способ модифицирования стали: Пат. 2781935 (РФ). 2022.
11. Pastor H. Titanium-carbonitride-based hard alloys for cutting tools. *Materials Science and Engineering: A*. 1988.105–106:401–409. https://doi.org/10.1016/0025-5416(88)90724-0
12. Askarova L.Kh., Grigorov I.G., Zainulin Yu.G. Liquid-phase interaction in the $TiC_{0.5}N_{0.5}$–TiNi–Ti system. *Metally*. 1998;(2):20–24. (In Russ.).

    Аскарова Л.Х., Григоров И.Г., Зайнулин Ю.Г. Жидкофазное взаимодействие в системе $TiC_{0.5}N_{0.5}$–TiNi–Ti. *Металлы*. 1998;2:20–24.
13. Askarova L.Kh., Shchipachev E.V., Ermakov A.N., Grigorov I.G., Zainulin Yu.G. Influence of vanadium and niobium on the phase composition of cermets based on carbide-titanium nitride with a titanium-nickel bond. *Neorganicheskie Materialy*. 2001;37(2):207–210. (In Russ.).

    Аскарова Л.Х., Щипачев Е.В., Ермаков А.Н., Григоров И.Г., Зайнулин Ю.Г. Влияние ванадия и ниобия на фазовый состав керметов на основе карбида – нитрида титана с титан-никелевой связкой. *Неорганические материалы*. 2001;37(2):207–210.
14. Askarova L.Kh., Grigorov I.G., Fedorenko V.V., Zainulin Yu.G. Liquid-phase interaction in $TiC_{0.5}N_{0.5}$–TiNi–Ti–Zr

and $TiC_{0.5}N_{0.5}$–TiNi–Ti–Zr alloys. *Metally*. 1998;(5): 16–19. (In Russ.).

Аскарова Л.Х., Григоров И.Г., Федоренко В.В., Зайнулин Ю.Г. Жидкофазное взаимодействие в сплавах $TiC_{0.5}N_{0.5}$–TiNi–Ti–Zr и $TiC_{0.5}N_{0.5}$–TiNi–Ti–Zr. *Металлы*. 1998;(5):16–19.

15. Askarova L.Kh., Grigorov I.G., Zainulin Yu.G. Liquid-phase interaction in $TiC_{0.5}N_{0.5}$–TiNi–Mo and $TiC_{0.5}N_{0.5}$–TiNi–Ti–Mo alloys. *Metally*. 1998;(6):24–27. (In Russ.).

Аскарова Л.Х., Григоров И.Г., Зайнулин Ю.Г. Жидкофазное взаимодействие в сплавах $TiC_{0.5}N_{0.5}$–TiNi–Mo и $TiC_{0.5}N_{0.5}$–TiNi–Ti–Mo. *Металлы*. 1998;(6):24–27.

16. Askarova L.Kh., Grigorov I.G., Zainulin Yu.G. Features of phase and structure formation during liquid-phase sintering of $TiC_{0.5}N_{0.5}$–TiNi–Nb and $TiC_{0.5}N_{0.5}$–TiNi–Ti–Nb alloys. *Metally*. 2000;(1):130–133. (In Russ.).

Аскарова Л.Х., Григоров И.Г., Зайнулин Ю.Г. Особенности фазо- и структурообразования при жидкофазном спекании сплавов $TiC_{0.5}N_{0.5}$–TiNi–Nb и $TiC_{0.5}N_{0.5}$–TiNi–Ti–Nb. *Металлы*. 2000;(1):130–133.

17. Sadovnikov S.I., Gusev A.I. Effect of particle size and specific surface area on the determination of the density of nanocrystalline silver sulfide Ag_2S powders. *Physics of the Solid State*. 2018;60:877–881. https://doi.org/10.1134/S106378341805027X

Садовников С.И., Гусев А.И. Влияние размера частиц и удельной поверхности на определение плотности нанокристаллических порошков сульфида серебра Ag_2S. *Физика твердого тела*. 2018;60(5):875–879. https://doi.org/10.21883/FTT.2018.05.45780.313

18. Bhaskar U.K., Pradhan S.K. Microstructural evolution of nanostructured Ti0.7Ni0.3N prepared by reactive ball-milling. *Materials Research Bulletin*. 2013;48:3129–3135. https://doi.org/10.1016/j.materresbull.2013.04.061

19. Bunaciu A.A., Udriştioiu E.G., Aboul-Enein H.Y. X-ray diffraction: Instrumentation and applications. *Critical Reviews in Analytical Chemistry*. 2015;45(4):289–299. https://doi.org/10.1080/10408347.2014.949616

20. Fultz B., Howe J.M. Transmission electron microscopy and diffractometry of materials, 3rd ed. Berlin, Heidelberg: Springer, 2008. 758 p. https://doi.org/10.1007/978-3-540-73886-2

Фульц Б., Хау Дж.М. Просвечивающая электронная микроскопия и дифрактометрия материалов. М.: Техносфера, 2011. 904 с. https://doi.org/10.1007/978-3-540-73886-2

21. Ermakov A.N., Luzhkova I.V., Avdeeva Yu.A., Murzakaev A.M., Zainulin Yu.G., Dobrinsky E.K. Formation of complex titanium-nickel nitride $Ti_{0.7}Ni_{0.3}N$ in the "core-shell" structure of TiN–Ni. *International Journal of Refractory Metals and Hard Materials*. 2019.84:104996. https://doi.org/10.1016/j.ijrmhm.2019.104996

22. Mhadhbi M., Driss M. Titanium carbide: Synthesis, properties and applications. *Brilliant Engineering*. 2021;2:1–11. https://doi.org/10.36937/ben.2021.002.001

23. Banaszek K., Klimek L. Wettability and surface free energy of Ti(C,N) coatings on nickel-based casting prosthetic alloys. *Archives of Foundary Engienering*. 2015;15:11–16. https://doi.org/10.1515/afe-2015-0050

24. Barin I. Thermochemical data of pure substances. 3rd ed. Weinheim, New York, Base1, Cambridge, Tokyo: VCH, 1995. 2003 c.

25. Gusev A.I., Rempel A.A. Nonstoichiometry, disorder and order in a solid. Ekaterinburg: NISO UrO RAN, 2001. 579 p. (In Russ.).

Гусев А.И., Ремпель А.А. Нестехиометрия, беспорядок и порядок в твердом теле. Екатеринбург: НИСО УрО РАН, 2001. 579 с.

26. Samokhin A.V., Polyakov S.N., Astashov A.G., Tsvetkov Yu.V. Simulation of the process of synthesis of nanopowders in a plasma reactor jet type. I. Statement of the problem and model validation. *Fizika i Khimiya Obrabotki Materialov*. 2013;(6):40–46. (In Russ.).

Самохин А.В., Поляков С.Н., Асташов А.Г., Цветков Ю.В. Моделирование процесса синтеза нанопорошков в плазменном реакторе струйного типа. I. Постановка задачи и проверка модели. *Физика и химия обработки материалов*. 2013;(6):40–46.

27. Samokhin A.V., Polyakov S.N., Astashov A.G., Tsvetkov Yu.V. Simulation of the process of nanopowder synthesis in a jet-type plasma reactor. II. Nanoparticles formation. *Inorganic Materials: Applied Research*. 2014;5(3): 224–229. https://doi.org/10.1134/S2075113314030149

Самохин А.В., Поляков С.Н., Асташов А.Г., Цветков Ю.В. Моделирование процесса синтеза нанопорошков в плазменном реакторе струйного типа. II. Формирование наночастиц. *Физика и химия обработки материалов*. 2014;(3):12–17. https://doi.org/10.1134/S2075113314030149

28. Shiryaeva L.S. Gorbuzova A.K., Galevsky G.V. Production and application of titanium carbide (assessment, trends, forecasts). *Nauchno-tekhnicheskie vedomosti Sankt-Peterburgskogo Gosudarstvennogo Universiteta*. 2014;2(195):100–107. (In Russ.).

Ширяева Л.С., Горбузова А.К., Галевский Г.В. Производство и применение карбида титана (оценка, тенденции, прогнозы). *Научно-технические ведомости Санкт-Петербургского государственного политехнического университета*. 2014;2(195):100–107.

29. Binder S., Lengauer W., Ettmayer P., Bauer J., Debuigne J., Bohn M. Phase equilibria in the systems Ti–C–N, Zr–C–N and Hf–C–N. *Journal of Alloys and Compounds*. 1995;217(1):128–136. https://doi.org/10.1016/0925-8388(94)01314-8

30. Moghimi Z.A., Halali M., Nusheh M. An investigation on the temperature and stability behavior in the levitation melting of nickel. *Metallurgical and Materials Transactions B*. 2006;37B:997–1005. https://doi.org/10.1007/BF02735022

31. Filkov M., Kolesnikov A. Plasmachemical synthesis of nanopowders in the system Ti(O,C,N) for material structure modification. *Journal of Nanoscience*. 2016;2016: 1361436. https://doi.org/10.1155/2016/1361436

32. Avdeeva Yu.A., Luzhkova I.V., Ermakov A.N. Mechanism of formation of nanocrystalline particles with core-shell structure based on titanium oxynitrides with nickel

in the process of plasma-chemical synthesis of TiNi in a low-temperature nitrogen plasma. *Nanosystems: Physics, Chemistry, Mathematics*. 2022;13(2):212–219. https://doi.org/10.17586/2220-8054-2022-13-2-212-219

33. Avdeeva Yu.A., Luzhkova I.V., Ermakov A.N. Formation of titanium-cobalt nitride $Ti_{0.7}Co_{0.3}N$ under plasma-chemical synthesis conditions in a low-temperature nitrogen plasma. *Nanosystems: Physics, Chemistry, Mathematics*. 2021;12(5):641–649. https://doi.org/10.17586/2220-8054-2021-12-5-641-649

34. Avdeeva Yu.A., Luzhkova I.V., Ermakov A.N. Plasmachemical synthesis of TiC–Mo–Co nanoparticles with a core–shell structure in a low-temperature nitrogen plasma. *Russian Metallurgy*. 2022;(9):1019–1026. https://doi.org/10.1134/s0036029522090038

Авдеева Ю.А., Лужкова И.В., Ермаков А.Н. Плазмохимический синтез наночастиц TiC–Mo–Co со структурой «ядро–оболочка» в низкотемпературной азотной плазме. *Металлы*. 2022;(5):41–49. https://doi.org/10.1134/s0036029522090038

Information about the Authors

Yuliya A. Avdeeva – Research Scientist at the Institute of Solid State Chemistry (ISSC) UB RAS
ORCID: 0000-0002-1470-0476
E-mail: y-avdeeva@list.ru

Irina V. Luzhkova – Research Scientist at the ISSC UB RAS
ORCID: 0000-0001-9123-5371
E-mail: key703@yandex.ru

Aidar M. Murzakaev – Cand. Sci. (Phys.-Math.), Senior Researcher at the Institute of Electrophysics UB RAS
ORCID: 0000-0003-4440-427X
E-mail: aidar@iep.uran.ru

Alexey N. Ermakov – Cand. Sci. (Chem.), Senior Researcher at the ISSC UB RAS
ORCID: 0000-0002-2746-5292
E-mail: ermakovihim@yandex.ru

Сведения об авторах

Юлия Александровна Авдеева – науч. сотрудник Института химии твердого тела (ИХТТ) УрО РАН
ORCID: 0000-0002-1470-0476
E-mail: y-avdeeva@list.ru

Ирина Викторовна Лужкова – науч. сотрудник ИХТТ УрО РАН
ORCID: 0000-0001-9123-5371
E-mail: key703@yandex.ru

Айдар Марксович Мурзакаев – к.ф.-м.н., ст. науч. сотрудник Института электрофизики УрО РАН
ORCID: 0000-0003-4440-427X
E-mail: aidar@iep.uran.ru

Алексей Николаевич Ермаков – к.х.н., ст. науч. сотрудник ИХТТ УрО РАН
ORCID: 0000-0002-2746-5292
E-mail: ermakovihim@yandex.ru

Contribution of the Authors

Yu. A. Avdeeva – processing the XRF and HR TEM results, participating in the discussion of the results.
I. ***V. Luzhkova*** – conducting experiments, participating in the discussion of the results.
A. M. Murzakaev – conducting HR TEM, processing the HR TEM results, participating in the discussion of the results.
A. N. Ermakov – determining the purpose of the work, conducting experiments, writing the article, participating in the discussion of the results.

Вклад авторов

Ю. А. Авдеева – обработка результатов РФА, ПЭМ ВР, участие в обсуждении результатов.
И. В. Лужкова – проведение экспериментов, участие в обсуждении результатов.
А. М. Мурзакаев – проведение ПЭМ ВР, обработка ПЭМ ВР, участие в обсуждении результатов.
А. Н. Ермаков – определение цели работы, проведение экспериментов, написание статьи, участие в обсуждении результатов.

Received 28.06.2023
Revised 16.11.2023
Accepted 20.11.2023

Статья поступила 28.06.2023 г.
Доработана 16.11.2023 г.
Принята к публикации 20.11.2023 г.